Chapter 12
Direct 3D Aerodynamic Optimization of Turbine Blades with GPU-Accelerated CFD

Philipp Amtsfeld, Dieter Bestle and Marcus Meyer

Abstract Secondary flow features of turbine blade flows are only assessable by 3D computational fluid dynamics (CFD) which is a time-consuming task. In this paper a fast automatic optimization process for the aerodynamic improvement of three-dimensional turbine blades is described and applied to a two-stage turbine rig. Basically, standard tools are used where the 3D CFD analysis, however, is significantly accelerated by a novel CFD solver running on graphics processing units (GPU) and the entire blade is parameterized in 3D. This approach shows that three-dimensional optimization of turbine blades is feasible within days of runtime and finds an improved blade design.

Keywords Turbine blade design · GPU flow solver · Shape optimization · Aerodynamic optimization · Parameter reduction

12.1 Introduction

Although turbomachinery aerodynamics has been already extensively improved over recent years, further optimization is still desirable to reduce emissions and fuel consumption. Typically, the aerodynamic design process of turbine blades is split into two phases: optimal design of 2D blade sections and then stacking them optimally along a three-dimensional stacking line. This separation of section design and stacking

P. Amtsfeld (✉) · D. Bestle
Engineering Mechanics and Vehicle Dynamics, Brandenburg University of Technology, Siemens-Halske-Ring 14, 03046 Cottbus, Germany
e-mail: philipp.amtsfeld@tu-cottbus.de

D. Bestle
e-mail: bestle@tu-cottbus.de

M. Meyer
Rolls-Royce Deutschland Ltd & Co KG, Eschenweg 11, 15827 Blankenfelde-Mahlow, Germany
e-mail: marcus.meyer@rolls-royce.com

D. Greiner et al. (eds.), *Advances in Evolutionary and Deterministic Methods for Design, Optimization and Control in Engineering and Sciences*, Computational Methods in Applied Sciences 36, DOI 10.1007/978-3-319-11541-2_12

is due to high computational costs of 3D flow simulation. Splitting the two phases reduces the number of design parameters and eases the design tasks. However, some loss mechanisms like secondary flow can only be assessed in 3D. Therefore, turbine blade design will be tackled as a real 3D problem in this paper.

Section design by automatic optimization processes is well-established since more than one decade [3, 4, 6, 13]. Various section parameterization approaches have been presented which are mainly based on physical design parameters and/or free form curves [5]. Flow simulation on stream surfaces is usually performed by Euler or Navier-Stokes solvers, where the former can be enhanced with a boundary layer model. Many kinds of optimization algorithms such as Evolutionary Algorithms have been used. Often the optimizer is coupled with a surrogate model to reduce the number of function evaluations.

There are also many reports about stacking optimization [1, 14]. Usually the sections are arranged in radial direction along the stacking line which is parameterized as a polynomial or free form curve. Keskin et al. [10] report on stacking optimization in an industrial environment with GPU-accelerated CFD.

Of course, also fully three-dimensional aerodynamic optimization has already been performed [9, 11, 12]. Blade parametrization or modification can be based on stacked sections, free form surfaces or free form deformation (FFD). These approaches are mainly limited by large number of design parameters and huge 3D evaluation time. If indicated, runtime of 3D blade optimization so far is in the order of many weeks.

In this work we present a fully 3D optimization of a turbine blade as part of a two-stage turbine research rig, where runtime is just a few days although hundreds of 3D design evaluations are performed. Aerodynamic design evaluation is significantly accelerated by a rapid flow solver running on GPUs. All computations run on a workstation equipped with four high-performance NVIDIA Tesla C2050 GPUs. Each of these GPUs offers 448 stream processors with up to 515 GFLOPs double precision peak computational power and 3 GB on-board memory. Apart from that the design process is built up from standard components. Design parameters are chosen according to a sensitivity analysis. The following sections describe the optimization problem, CFD analysis, parameterization, parameter reduction and optimization results.

12.2 Problem Formulation

The main goal in aerodynamic turbine blade design is to maximize the component efficiency η:

$$\max_{\mathbf{p}_l \le \mathbf{p} \le \mathbf{p}_u} \eta. \tag{12.1}$$

However, this is constrained by keeping given operation conditions and engine properties like inlet capacity $\dot{m}_{\text{cor}}^{\text{ref}}$ and degrees of reaction ρ_1^{ref} and ρ_2^{ref} of both stages of the considered two-stage turbine which are set in preliminary design phases:

$$\begin{aligned} \dot{m}_{\text{cor}} &= \dot{m}_{\text{cor}}^{\text{ref}} \\ \rho_1 &= \rho_1^{\text{ref}} \\ \rho_2 &= \rho_2^{\text{ref}}. \end{aligned} \tag{12.2}$$

Inlet capacity is associated with the mass flow at turbine inlet. Usually the inlet capacity determines the mass flow through the whole turbomachine and is kept fixed in this design phase. The degree of reaction of a turbomachinery stage is defined as fraction of fluid temperature drop across the rotor in relation to the temperature drop of the corresponding stage. This is a measure for the fluid work on the rotor and related to axial bearing loads. Thus, the reactions might affect other engine components which is why they may not be changed.

More constraints, e.g. on geometry or aerodynamics would be applicable, too. However, this is omitted here to keep problem formulation and CFD post-processing as simple as possible. For simplification of numerical optimization, constraints (12.2) are only enforced to be fulfilled within small tolerances ε_i, i.e.,

$$\begin{aligned} \left|\dot{m}_{\text{cor}} - \dot{m}_{\text{cor}}^{\text{ref}}\right| &\leq \varepsilon_0, \\ \left|\rho_1 - \rho_1^{\text{ref}}\right| &\leq \varepsilon_1, \\ \left|\rho_2 - \rho_2^{\text{ref}}\right| &\leq \varepsilon_2. \end{aligned} \tag{12.3}$$

The constrained scalar optimization problem (12.1), (12.3) may then be solved with a penalty strategy. The blade parameterization and choice of design parameters is explained in more detail in Sect. 12.4.

12.3 CFD Analysis with a GPU-Accelerated Flow Solver

In this work, CFD analyses are performed with the fast flow solver Turbostream [2] which is a massively parallel re-implementation of an existing CFD solver for flows in turbo-machinery to optimally run on modern multi-core hardware like high-performance GPUs. Turbostream solves the Reynolds-averaged Navier-Stokes (RANS) equations with the finite volume method in cylindrical polar coordinates. Turbulence is modeled by a mixing length model and wall shear stresses are computed with a wall function. Unsteady multi-stage effects are modeled with a mixing plane approach.

Boundary conditions are specified by radial distributions of total pressure $P_I(r)$, total temperature $T_I(r)$, yaw angle $\alpha_t(r)$ and pitch angle $\alpha_r(r)$ at the inlet and by

Fig. 12.1 Computational domain of the investigated turbine with boundary conditions at inlet and exit

static pressure distribution $p_E(r)$ at the exit, see Fig. 12.1. Extra inlet patches are used for film cooling and cooling flows at the hub cavities and trailing edge slots. The initial flow field is generated from rough aerodynamic data based on preliminary design.

The structured mesh has a multi-block topology with arbitrary patches. In general, a HOH mesh topology is used for each blade. On the blade surface, y+ values are in the order of 20. Furthermore, geometric features like fillets, stub cavities, trailing edge slots and tip gaps are represented by the mesh. The resulting mesh generated by the rapid Rolls-Royce in-house meshing system PADRAM [15] has 2.6 million cells for four blade rows. This mesh size fits into the memory of one GPU card used for this project. Thus four CFD analyses may be performed in parallel on the machine described in Sect. 12.1.

12.4 Parametric Blade Model

Parameterization is a key driver for successful optimization. The concept of the three-dimensional blade description chosen here is based on sections which are defined on stream surfaces at several radial heights from hub to casing, see Fig. 12.2a. Each section is defined by circular arc segments for the leading and trailing edge, respectively, and B-splines for suction and pressure side, respectively. Typical section parameters are the chord length c, stagger angle ξ, metal angles β_j, wedge angles μ_j, circle radii r_j, tangential spline control points t_j^k and free spline control points $(s_i^k;\ n_i^k)$, Fig. 12.2b, where $j \in \{I, E\}$ denotes inlet or exit, $k \in \{S, P\}$ marks suction or pressure side and i is a numbering of spline control points. This concept is implemented as an industrial parametric blade design tool [7]. In this case, the suction and pressure side are defined with four and two free control points, respectively.

The radial height of every section is determined by the stream surface it is defined on. To account for optimal stacking, a section can be moved on its stream surface

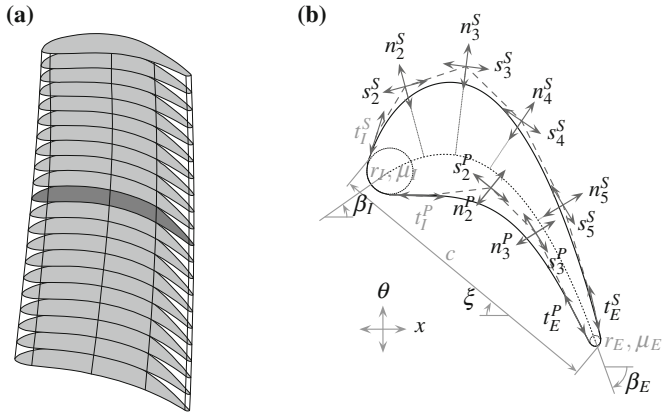

Fig. 12.2 Turbine blade consisting of stacked sections (**a**) and a parameterized section (**b**). Labels of section parameters which are not modified in this investigation are colored in *gray*

in axial and circumferential directions by axial shift x and circumferential shift θ, respectively. The three-dimensional blade is then obtained by arranging the sections above each other and interpolating the section shapes.

So far, section design and stacking would be described separately. For a three-dimensional parametric blade model the section parameters need to be coupled in a proper way to fulfill two goals:

- the output of the parametric model shall be compatible with an existing blade and section storage system
- the resulting blade shape shall be smooth.

In order to achieve this, the change of every section parameter $\Delta \bullet (\tilde{r})$ along the normalized radial coordinate $\tilde{r}$ relative to a reference design is parameterized with a second-order B-spline with an arbitrary number of control points. The first and last control point can move only along hub ($\tilde{r} = 0$) and casing ($\tilde{r} = 1$), respectively, whereas the others are free to move in both directions, Fig. 12.3. Usually only three control points are used for each section parameter described above. However, circumferential shift is parameterized with five control points as it is considered to be important and to allow for more design freedom.

These moves of the control points are used as design variables summarized in the design vector $\mathbf{p}$ of problem formulation (12.1) and limited by lower and upper bounds $\mathbf{p}_l$ and $\mathbf{p}_u$, respectively. The parametric model requires that the reference design is already smooth and roughly adapted to flow conditions. Changed design parameters are translated to modified sections which are saved, converted to a three-dimensional blade and passed to the meshing system and CFD analysis (Sect. 12.3).

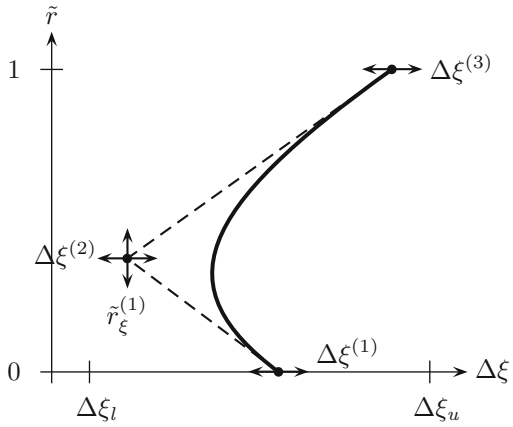

Fig. 12.3 Exemplary radial parameterization of the change of stagger angle $\Delta\xi$ relative to the reference design by a B-spline with three control points

12.5 Parameter Reduction

The used 3D parametric model has much more degrees of freedom than could reasonably be handled in a direct optimization. In order to decide on the most important parameters, a design of experiments (DoE) with Optimal Latin Hypercube sampling is performed. The varied parameters are the control points of the radial B-splines determining changes of axial and circumferential shifts, stagger angle, metal angles, free control points of suction and pressure side and tangential control points at the trailing edge. In total this yields 76 design parameters. 500 design evaluations are performed within 2.4 days, where four evaluations are computed in parallel in approximately 40 min and 82 % of the designs are analysed successfully.

Based on these DoE results a sensitivity analysis is performed to assess the influence of every design parameter on the objective and the constraints. Due to the large number of parameters and relatively small number of samples, the Spearman correlation coefficient is used. It provides a measure for the monotone dependence between two sampled variables.

According to Fig. 12.4a, turbine efficiency shows the strongest correlations with changes to circumferential and axial shifts and free control points on suction side. Free control points on pressure side and exit metal angle have smaller influence. Inlet metal angle and tangential control points only have insignificant correlations. Inlet capacity is mostly influenced by variations of stagger angle, free control points on suction side near the throat and exit metal angle, Fig. 12.4b. Changes of tangential shift and others have small influence on inlet capacity.

A similar interpretation can be done for the degrees of reaction of both stages, Fig. 12.5. The reaction of stage 1 also has the strongest correlation with changes to stagger angle, free control points on suction side near the throat and exit metal angle. Reaction of stage 2 is mostly influenced by changes of tangential shift, free control

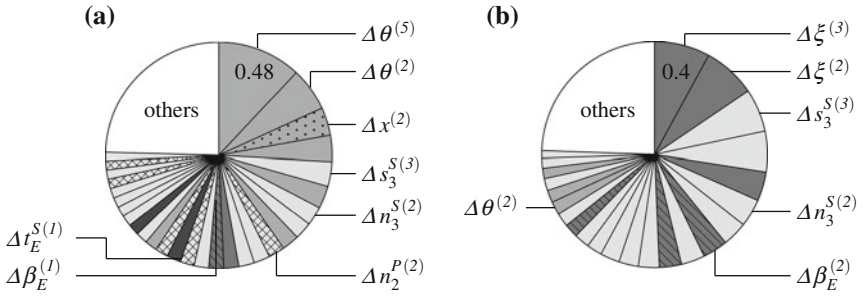

Fig. 12.4 Normalized absolute values of Spearman correlation coefficients as measure of correlation between exemplary design parameters and (**a**) turbine efficiency and (**b**) inlet capacity

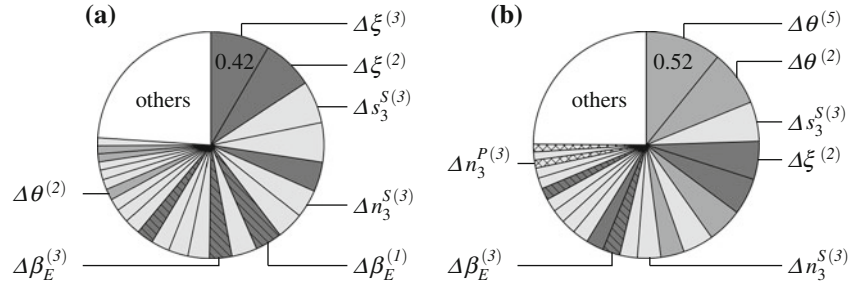

Fig. 12.5 Normalized absolute values of Spearman correlation coefficients as measure of correlation between exemplary design parameters and reaction of (**a**) stage 1 and (**b**) stage 2

points on suction side and stagger angle. A small correlation can be noticed for exit metal angle.

Consequently, parameters associated to changes of inlet metal angle, tangential control points and control points on the pressure side seem to have only small influence on the objective and constraints. Therefore, the 28 parameters associated with these quantities will not be used as design parameters in the following optimization runs.

12.6 Optimization

The automated aerodynamic design evaluation can be employed in an optimization process. For optimization the algorithm CMA-ES [8] is used which is a stable, derivative-free, black box evolution strategy for unconstrained single-objective problems. Its most important property is the de-randomized change of strategy parameters which means that they are adapted deterministically. The step-size σ is adapted based on the evolution path of previous generations. Themulti-variate

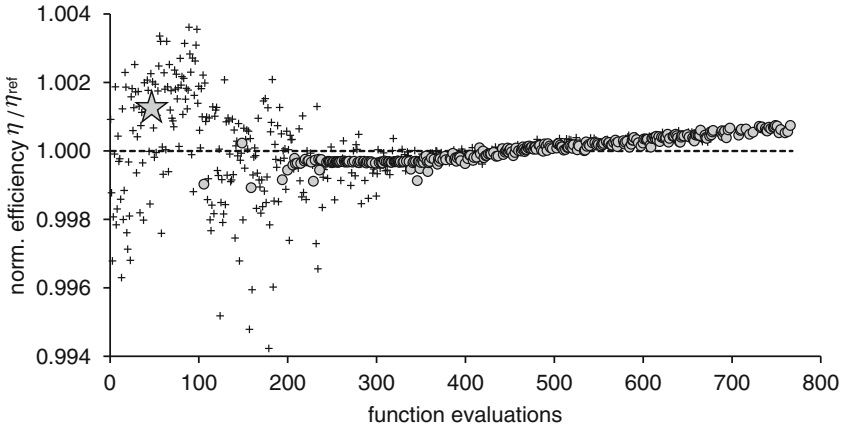

Fig. 12.6 Efficiency of optimal (⋆), feasible (○) and infeasible (+) designs relative to baseline

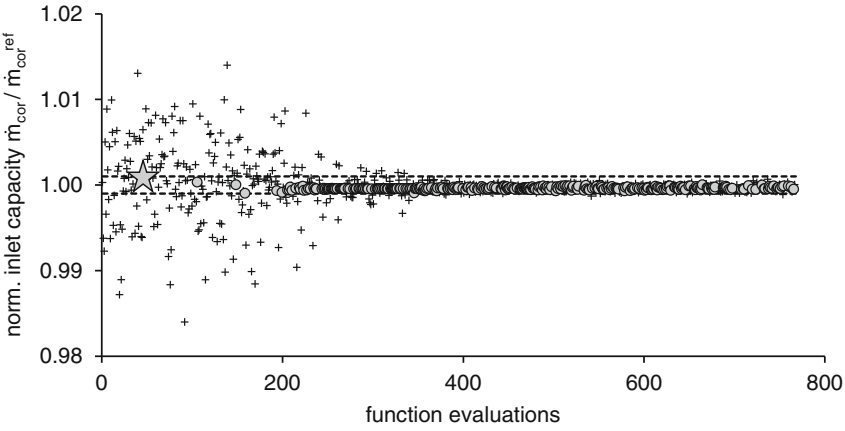

Fig. 12.7 Inlet capacity of optimal (⋆), feasible (○) and infeasible (+) designs relative to baseline

normal search distribution is controlled by an adapted covariance matrix of successful previous designs. Furthermore, CMA-ES has some invariance properties which make it very robust.

Based on the sensitivity analysis in Sect. 12.5, the selected design parameters for optimization are associated with axial and circumferential shifts, stagger angle, exit metal angle and free control points of suction side. This yields 48 design parameters of the 3D blade model. The population size of CMA-ES is reduced from the default value of 13 to 12 to optimally exploit parallel evaluation capability of the used GPU workstation. Several optimization runs were performed where Figs. 12.6 and 12.7 represent a typical result.

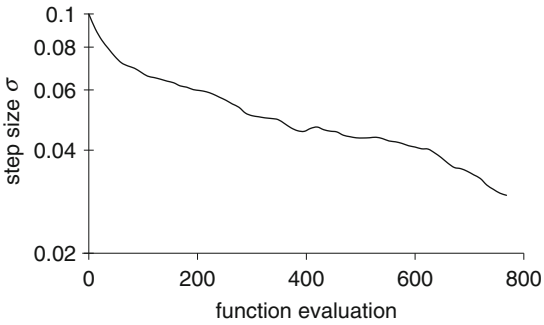

Fig. 12.8 Step size σ of CMA-ES during optimization

In total 768 design evaluation respectively 64 generations are performed in four and a half days. The optimization is terminated prematurely when the maximum number of generations is reached. All design evaluations converge where 40.7 % are feasible w.r.t. the optimization constraints (12.3). In the first 400 iterations large variations in objective and constraints can be observed. After that the optimization algorithm has reduced its step-size to a more successful order (Fig. 12.8) and begins to converge which results in a further decreasing step size, increased number of feasible designs and a continuous improvement of efficiency. The finally best feasible design ($\star$) is found in the early phase already. However, if the optimization runs longer, the optimization will converge and reach such an efficiency level again.

The optimal design is shown in Fig. 12.9. It fulfills the constraints (12.3) and has a slightly improved efficiency. Major design changes are that the tip section is moved

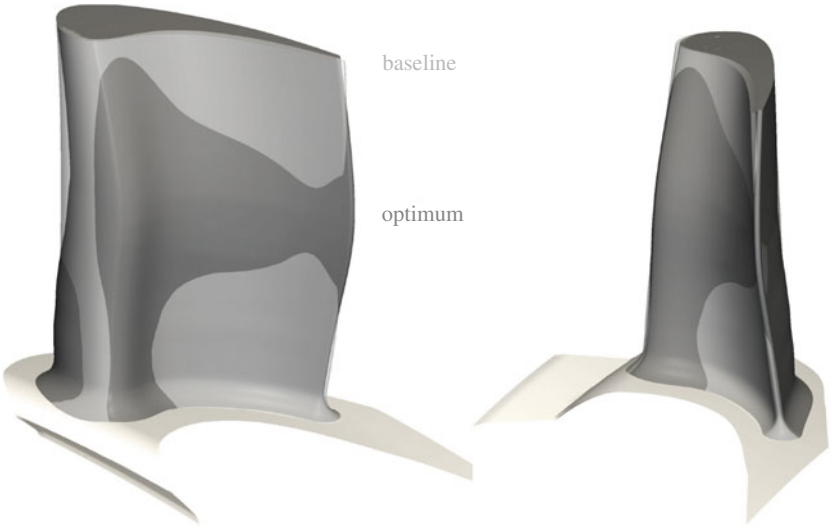

Fig. 12.9 Two views of a comparison between the blade shapes of baseline (*light grey transparent*) and optimal (*dark gray*) design

in circumferential direction of the suction side whereas the midsection is moved towards the opposite direction. In addition to the modifications of the stacking there are also significant modifications of the section parameters like a varying increase of the exit metal angle along the blade height or an decrease of the stagger angle.

12.7 Conclusions

A fast optimization process for the aerodynamic improvement of three-dimensional turbine blades is achieved by assessing the aerodynamic quality of a multi-stage turbine by a novel CFD solver running on GPUs. Wall-clock time of one 3D CFD is reduced to approximately 40 min, however, further speed-up is achieved by parallel design evaluation using multiple GPUs. Only standard tools are used for optimization, mesh generation and blade modification, where the three-dimensional blade parameterization is based on a well-known section parameterization. This allows to implement the proposed design approach in an industrial design environment.

A consequence of three-dimensional blade parameterization is the large number of design parameters. Therefore, a DoE is performed on all appropriate blade parameters and the design vector for optimization can be reduced to 48 design variables showing most significant influence on objective and constraints assessed by Spearman correlation coefficients. The optimization is characterized by a large variation of constraint values at the beginning and a steady improvement of efficiency after that. All optimization runs are terminated prior to convergence when the maximum number of generations is reached. Nevertheless, this paper shows that a fully three-dimensional optimization of turbine blades is feasible within days of runtime and finds improved blade designs.

Acknowledgments This work has been carried out in collaboration with Rolls-Royce Deutschland as part of the research project VIT 3 (Virtual Turbomachinery, contract no. 80142272) funded by the State of Brandenburg, the European Community and Rolls-Royce Deutschland. Rolls-Royce Deutschland's permission to publish this work is greatly acknowledged.

References

1. Arabnia M, Ghaly W (2009) A strategy for multi-point shape optimization of turbine stage in three-dimensional flow. In: Proceedings of ASME turbo expo 2009, GT2009-59708, Orlando, Florida
2. Brandvik T, Pullan G (2011) An accelerated 3D Navier-Stokes solver for flows in turbomachines. J Turbomach 133(2):021025
3. Briasco G, Cravero C, Macelloni P (2010) Turbine blade profile optimization using soft-computing techniques. In: Proceedings of 2nd international conference on engineering optimization, Lisbon, Portugal
4. Dennis B, Egorov I, Han ZX, Dulikravich G, Poloni, C (2000) Multi-objective optimization of turbomachinery cascades for minimum loss, maximum loading, and maximum gap-to-chord

ratio. In: Proceedings of 8th AIAA/NASA/USAF/ISSMO symposium on multidisciplinary analysis and optimization, AIAA 2000-4876, Long Beach, California
5. Ghaly W (2010) Shape representation. In: North Atlantic treaty organization, research & technology organization (ed) strategies for optimization and automated design of gas turbine engines, RTO-EN-AVT-167
6. Giannakoglou KC (1999) Designing turbomachinery blades using evolutionary methods. In: Proceedings of 44th ASME gas turbine & aeroengine congress, 9-GT-181, Indianapolis
7. Gräsel J, Keskin A, Swoboda M, Przewozny H, Saxer A (2004) A full parametric model for turbomachinery blade design and optimisation. In: Proceedings of ASME DETC 2004, DETC2004-57467, Salt Lake City, Utah
8. Hansen N, Ostermeier A (2001) Completely derandomized self-adaptation in evolution strategies. Evol Comput 9(2):159–195
9. Hasenjäger M, Sendhoff B, Sonoda T, Arima T (2005) Three dimensional aerodynamic optimization for an ultra-low aspect ratio transonic turbine stator blade. In: Proceedings of ASME turbo expo 2005, GT2005-68680, Reno-Tahoe, Nevada
10. Keskin A, Haselbach F, Meyer M, Janke E, Brandvik T, Pullan G (2011) Aerodynamic design and optimzation of turbomachinery component using a GPU flow solver. In: Proceedings of 9th European conference on turbomachinery fluid dynamics and thermodynamics, Istanbul, Turkey
11. Menzel S, Olhofer M, Sendhoff B (2006) Evolution design optimisation of a turbine stator blade using free form deformation techniques. In: Proceedings of conference on modelling fluid flow (CMFF'06), Budapest, Hungary
12. Nagel MG (2004) Numerische Optimierung dreidimensional parametrisierter Turbinenschaufeln mit umfangsunsymmetrischen Plattformen—Entwicklung, Anwendung und Validierung. PhD thesis, Universität der Bundeswehr München
13. Pierret S, Van den Braembussche RA (1999) Turbomachinery blade design using a navier-stokes solver and artificial neural network. J Turbomach 121(2):326–332
14. Pierret S, Demeulenaere A, Gouverneur B, Van den Braembussche RA (2000) Designing turbomachinery blades with the function approximation concept and the navier-stokes equations. In: Proceedings of 8th AIAA/USAF/NASA/ISSMO symposium on multidisciplinary analysis and optimization, AIAA 2000-4879, Long Beach, California
15. Shahpar S, Lapworth L (2003) Padram parametric design and rapid meshing system for turbomachinery optimisation. In: Proceedings of ASME turbo expo 2003, GT2003-38698, Atlanta, Georgia, pp 579–590